33RD INTERNATIONAL COSMIC RAY CONFERENCE, RIO DE JANEIRO 2013
THE ASTROPARTICLE PHYSICS CONFERENCE

ICRC 2013

Microwave Emission due to Molecular Bremsstrahlung in Non-Thermal Air Shower Plasmas

PATRICK NEUNTEUFEL[1], SEBASTIAN BAUR[1], RALPH ENGEL[1], JAN PEKALA[2] RADOMIR SMIDA[1], JAROSLAV STASIELAK[1,2], FELIX WERNER[1], HENRYK WILCZYNSKI[2]

[1] *Karlsruhe Institute of Technology (KIT), Germany*
[2] *Institute of Nuclear Physics (INP), Cracow, Poland*

ralph.engel@kit.edu

Abstract: The observation of microwave signals due to molecular bremsstrahlung in the plasma of ionization electrons and neutral atoms formed by air showers could provide a new method of detecting ultra-high energy air showers. Several experiments were built to search for these microwave signals, for example AMBER, MIDAS, EASIER, and CROME. The expected microwave yield is not yet known as there are contradicting laboratory measurements. Here we present a theoretical calculation of the expected microwave intensity for the extremely short lived and non-thermal plasma produced by the shower particles in air. We predict the microwave intensity for different shower-observer geometries including observation from a large distance perpendicular to the shower axis (AMBER, MIDAS) and observation near the Cherenkov angle. The calculation includes the effects of signal amplification due to the time compression of the observed shower signal at angles close to the Cherenkov angle and due to the density-dependent lifetime of the plasma.

Keywords: extensive air showers, microwave radiation, molecular bremsstrahlung, plasma physics.

1 Introduction

Due to the low flux of cosmic ray particles at the highest energies, properties of these particles such as energy and primary particle type (mass) have to be estimated from extensive air showers (EAS) they produce in the atmosphere. The measurement of showers is either based on particle detection using a surface detector array or observation with Cherenkov or fluorescence telescopes [1]. Fluorescence telescopes are optimized to detect the fluorescence light emitted by nitrogen molecules of the atmosphere excited by high energy shower particles. They allow the measurement of the longitudinal shower profile and provide currently the best means of measuring calorimetrically the primary energy and determining the mass composition. While this detection method has been used in recent years with great success, it has proven highly sensitive to environmental conditions and is characterized by a duty cycle of about 15%.

To supplement fluorescence detection, observations of air shower emissions in different regions of the electromagnetic spectrum were proposed and successfully undertaken. In 2008 Gorham *et al.* proposed the observation of EAS in the microwave range of the electromagnetic spectrum [2]. The proposed dominant emission mechanism for this radiation is free-free interactions of very low energy electrons, forming a weakly ionized plasma in the wake of the higher energy shower front, with neutral atmospheric molecules. Radiation emitted via this process, dubbed the molecular bremsstrahlung mechanism, would, as argued by Gorham *et al.*, have a number of desirable properties: The radiation would be 1. isotropic, facilitating observations akin to nitrogen fluorescence detection, 2. subject to very little atmospheric absorption, 3. in a frequency range of very little background, natural or other. In the time since the first proposal of measuring microwave emission by EAS, a number of air shower and beam experiments – AMBER, MIDAS, EASIER, CROME, MAYBE, AMY – have been performed. These measurements, most notably by the EASIER [3] and CROME [4] groups, while able to verify the emission of microwave radiation at measurable intensities by EAS, do not currently support the notion of molecular bremsstrahlung being the dominant emission mechanism. In this paper, a mathematical description of the theoretical model proposed by Gorham *et al.* as well as the findings of a simulation framework based on it are presented. The findings are then discussed with regard to their implications for the hypothetical detectability of an EAS microwave signal produced via the molecular bremsstrahlung mechanism.

2 Air Shower Plasma Production

The expected signal is heavily dependent on the assumed conditions within the emitting plasma. These conditions, again, depend on the exact mechanism of plasma production. The very low energy part of the shower ensemble, which is assumed to be responsible for the emission of molecular bremsstrahlung radiation, is not well understood. However, under the assumption that a majority of low energy electrons are produced through ionization of the surrounding atmosphere, a number of parameterizations of numerical shower simulations may be used in order to derive an estimate of the low energy electron spectrum. The longitudinal profile of the shower can be parameterized using a Gaisser-Hillas formula with numerically calculated parameters [5], here in the form

$$N(X - X_1) = N_{\max} \left(\frac{X - X_0}{X_{\max} - X_0} \right)^{\left(\frac{X_{\max} - X_0}{\Lambda} \right)} \exp\left(\frac{X_{\max} - X}{\Lambda} \right) \quad (1)$$

where X is the atmospheric depth, $X_{\max}$ is the depth of shower maximum, and X_0, X_1, and Λ are fitting parameters.

Of further importance is the velocity distribution of the shower particles. We use a parameterization of energy distributions obtained numerically through the CORSIKA code [6], which may be written as

$$f'_e(X,E) = a_0 \cdot \frac{E}{(E+a_1)(E+a_2)^s}, \tag{2}$$

where a_0, a_1, and a_2 are functions consisting of individual fitting parameters and are dependent on the shower age, denoted by s. The shower lateral distribution is derived, under the assumption of constant energy distribution over the entire lateral expanse of the shower (which, strictly speaking, is not correct), from a numerical parameterization of the energy deposit of the shower. The parameterization, taken from Gora *et al.* [7], can be written as

$$F(r^*) = 1 - (1 + a(s)r^*)^{-b(s)}, \tag{3}$$

where $a(s)$ and $b(s)$ are fitting functions dependent on s. Together, these parameterizations fully characterize the shower particles, including their energy distribution, at any point of its longitudinal and lateral distribution. This initial distribution is then used, together with a doubly differential Mott cross section to calculate the distribution of the low energy region of the plasma. It should be emphasized at this point that a Mott cross section is only a crude approximation, which is nevertheless necessary due to the unavailability of doubly differential ionization cross sections for any elements heavier than Helium, let alone molecules of any kind. The cross section [8] can be written as

$$\frac{\mathrm{d}\sigma}{\mathrm{d}Q} = \frac{2\pi z^2 \alpha^2 \hbar^2}{\beta^2 m_e} \frac{1}{Q^2} \left[1 - \beta^2 \frac{Q}{Q_{\max}} + \frac{1}{2} \left(\frac{Q}{E + mc^2} \right)^2 \right], \tag{4}$$

where Q is the transferred energy, α the fine structure constant. The resulting energy distribution has no analytic representation, but is roughly exponential in shape. A graphic representation of some numerically calculated distributions are depicted in Fig. 1. This can then be combined to calculate the density as well as the energy distribution of the plasma. It was found that the density profile can be fitted to a Gaisser-Hillas-like function, giving the plasma density instead of the total particle count as a function of shower depth. It is a striking result that point of highest plasma density does not correspond with the point of maximum particle count as described by the Gaisser-Hillas function of the high energy component of the shower. This effect is due to the changing energy distribution of the shower particles in relation to the ionization cross section.

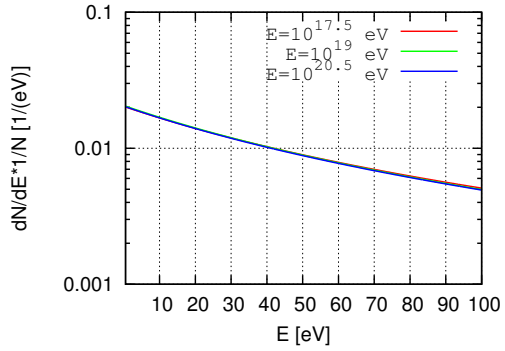

Figure 1: Graphical representation of the electron energy distributions as expected for electrons ionized by an incident distribution as described by Eq. (4) and Eq. (2). The plot shows the expected distribution expected at shower age $s = 1$ for vertical showers of different energies. The differences between the curves is very small and almost impossible to see in this presentation.

In order to calculate the radiation emitted by a decaying plasma, it is necessary to make a statement about its expected lifetime. The two most prominent mechanisms for the removal of electrons from the plasma are electron attachment and recombination [9]. In the atmospheric region of interest, the lower atmosphere, also due to the involved plasma densities, electron attachment dominates [10]. The attachment rate is dependent on the particle density of the atmospheric elements involved through

$$\frac{\partial N_e}{\partial t} = -k_{\mathrm{att1}} N_e N_m^2 [O_2]^2 - k_{\mathrm{att2}} N_e N_m^2 [O_2][N_2] \tag{5}$$

where N_e is the electron number density, N_m is the total number density of atmospheric molecules (Nitrogen, Oxygen, Carbon-Dioxide and trace gases), $[O_2]$ is the fraction of Oxygen and $[N_2]$ the fraction of Nitrogen in the atmosphere. The latter two are taken to be

$$[N_2] = 0.78084,\ [O_2] = 0.209476$$

The attachment coefficients are

$$k_{\mathrm{att1}} = 2 \cdot 10^{-30} \mathrm{cm}^6 \mathrm{s}^{-1},\ k_{\mathrm{att2}} = 8 \cdot 10^{-32} \mathrm{cm}^6 \mathrm{s}^{-1}.$$

This leads to an expected plasma lifetime ~ 15 ns at sea level, increasing significantly at higher altitudes within the region of interest, as seen in Fig. 2.

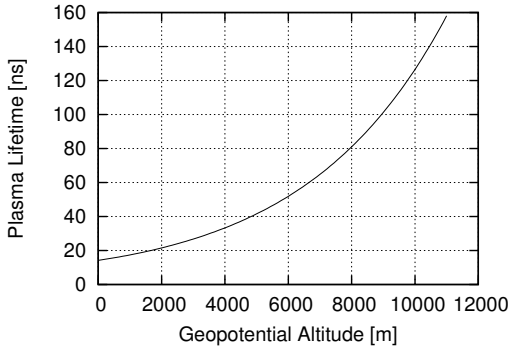

Figure 2: Expected lifetime of plasma with respect to altitude.

3 Theory of Molecular Bremsstrahlung

Using the toolkit described in the previous section, the local density, as well as the energy distribution of the low energy plasma produced by an EAS can be derived. The expected intensity of the emitted signal can then be calculated. The following short description is based on a thorough discussion of plasma radiation phenomena in [11].

The intensity emitted by a radiating volume of plasma can be expressed as

$$\frac{\mathrm{d}}{\mathrm{d}\tau} \left(\frac{I_\omega}{n_r^2} \right) = \frac{I_\omega}{n_r^2} - S_\omega, \tag{6}$$

where I_ω is the intensity of radiation emitted with radian frequency ω, τ is the optical depth and n_r is the refractive index along the line of sight between the point of emission and the observer. S_ω is called "source function", which is defined as

$$S_\omega = \frac{1}{n_r^2}\frac{j_\omega}{\alpha_\omega}, \tag{7}$$

where

$$j_\omega = \frac{N_a e^2}{24\pi^3\varepsilon_0 c^3}\int_0^\infty \sigma_m(v) f(v) v^5\,\mathrm{d}v \tag{8}$$

is the emission coefficient and

$$\alpha_\omega = -\frac{4\pi}{3c}\frac{\omega_p^2 N_a}{\omega^2}\int_0^\infty \sigma_m(v)\frac{\partial f}{\partial v} v^4 \mathrm{d}v \tag{9}$$

the absorption coefficient. In both equations, v is electron speed, ω_p is the radian plasma frequency, N_a is the target particle density, f is the velocity distribution of the plasma, c is the speed of light, e the elementary charge, ε_0 is the vacuum permittivity, ω the radian frequency of the emitted radiation and σ_m is the momentum transfer cross section of each target particle species. The value of each of the parameters can be obtained through application of the arguments presented in Sec. 2, with the exception of the momentum transfer cross section. As of the time of writing, analytical representations of the desired momentum transfer cross sections at low energy of at least molecular oxygen and molecular nitrogen have not been forthcoming, leaving utilization of experimental values as the only way forward. Fig. 3 shows the values for momentum transfer cross sections of oxygen and hydrogen published in [12] and [13].

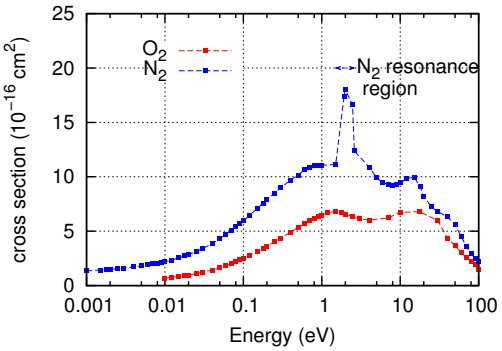

Figure 3: Momentum cross sections of molecular oxygen and nitrogen at low incident electron energies. The cross section of molecular nitrogen in the resonance region, as indicated, is plotted at its best estimate.

It should be noted that only Eq. (9) is directly dependent on the frequency of the emitted radiation. Solving Eq. (6) and integrating with respect to τ to a small physical length, l, then expanding the result with respect to α_ω yields

$$I_\omega = \frac{j_\omega \cdot l}{n(\omega)^2}. \tag{10}$$

This means that if α_ω is small, the intensity of the emitted radiation is independent of its frequency, modified only by the frequency dependence of the refractive index of the traversed medium. This condition is fulfilled, due to the plasma densities and radiation frequencies involved, for microwave emissions of air showers of energy smaller than $10^{18.5}$ eV.

These descriptions omit the modification of the signal due to plasma dispersion, which introduces a frequency dependent factor into the nominator of Eq. (8) as well as Eq. (9). Every result shown in Sec. 4 should therefore be understood as an upper limit.

4 Results

Due to the occurrence of a number of analytically unsolvable integrals, the implications of the theoretical considerations sketched out above have to be explored using numerical methods in the form of a simulation framework. For a detailed description of the simulation framework, the reader is referred to [14].

The methodology of the framework can be summarized as follows: The volume traversed by the shower is broken up into small, rectilinear volumes/cells. Using the descriptions outlined in Sec. 2, the density of the plasma and its energy distribution in each cell are determined for all relevant times. Then, using the descriptions presented in Sec. 3, the intensity of radiation emitted by each cell is calculated. The radiation is then propagated through each plasma-filled cell lying between the point of emission and a chosen observer, all the while respecting the influence of the partially ionized medium on the signal. The simulation is therefore three-dimensional as well as capable of handling time inversions of the signal and Cherenkov-like beaming effects.

Due to the excessive demands placed on processing hardware by this simulation, optimization of the code notwithstanding, economical usage of processing time is mandatory. All results presented in this section are therefore computed for the case of a vertical proton induced EAS of energy $E = 10^{17.5}$eV. This particular shower was chosen in order to facilitate comparison with the expected values presented in [2].

Two distinct cases are considered, as far as detectability by different kinds of experiments is concerned: MIDAS-like [3] and CROME-like [4]. Since the CROME set up is oriented vertically and near vertically upward, most showers crossing the field of view, possessing a near to vertical orientation themselves, will impact the ground relatively closely to the receiver. MIDAS, on the other hand, being oriented close to the horizontal, would have showers crossing its field of view at larger distances as well, but would be unable to take advantage of any signal compression at small angles to the shower axis. A number of signal traces, given in units of spectral energy flux density, inside the CROME-like region, taken to extend between $d = 0$ m and $d = 500$ m between observer and the point of shower core impact, are shown in Fig. 4. The time coordinate is defined as $t = 0$ at the point where the shower crosses $s = 0.7$.

Two points of insight may be gained from this plot: 1. In the case of proton showers, the expected intensity is monotonically falling with increasing distance from the point of shower impact 2. The overall signal produced via the molecular bremsstrahlung mechanism is at least four orders of magnitude lower than the signal expected from geomagnetic emission [4]. Furthermore, due to the short lifetime of the plasma, the effects of the geomagnetic field

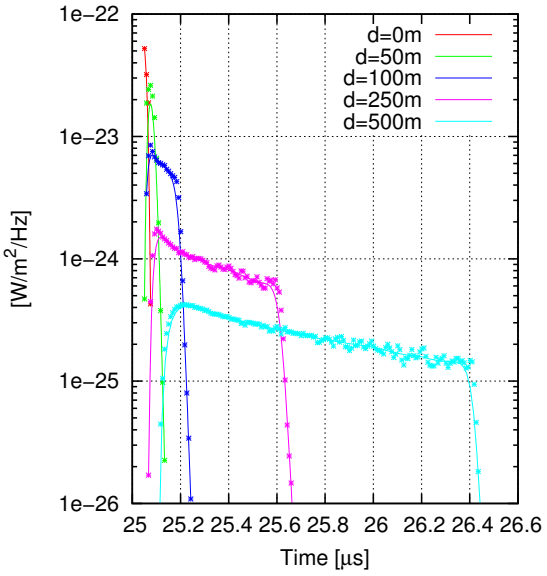

Figure 4: Expected signal traces given in units of spectral energy flux density at most likely distances for CROME-like events. The time coordinate is chosen such that $t = 0$ at the point where the shower crosses $s = 0.7$.

will be minimal, the decrease of the signal can be assumed to be radially symmetric.

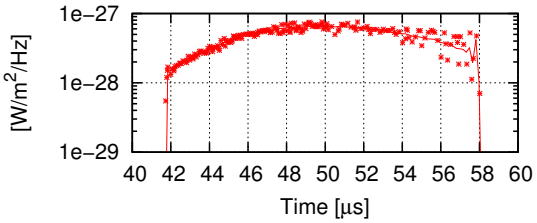

Figure 5: Expected signal trace given in units of spectral energy flux density at most likely distances for a MIDAS-like event. The distance from shower impact is $d = 10$ km. The time coordinate is chosen such that $t = 0$ at the point where the shower crosses $s = 0.7$. The divergence at later times is due to slight geometric instabilities caused by large cell sizes.

Fig. 5 shows the expected signal for the case of MIDAS-like showers. The divergence at later times is due to geometric instabilities caused by large cell sizes. It should be mentioned, that these values are on the order three magnitudes lower and therefore in contradiction to the minimal signal strengths derived in [2], but that the values shown in Fig. 4 are in good agreement with the measurements taken by the CROME group as shown in [4].

It ought to be mentioned that, since the expected signal strength scales with plasma density, the energy deposit per created electron-ion pair is predicted by the considerations in Sec. 2 to be about 133 eV, while [10] cites a value of about 33.8 eV. The results presented in this section can be rescaled to match that value, increasing the signal strengths by about one order of magnitude. The conclusions drawn from the simulations remain largely unaffected by this change.

5 Conclusions

We have carried out a theoretical calculation of the signal expected from air showers due to molecular bremsstrahlung. For the first time a non-thermal electron energy distribution has been considered. Also the density-dependent lifetime of the electron plasma has been accounted for. No non-linear amplification of the molecular bremsstrahlung signal due to coherence effects is found in our approach. From the results of our simulations and the theoretical considerations outlined here, we draw the following conclusions.

1. There are significant differences in signal characteristics between microwave radiation produced by the molecular bremsstrahlung and the geomagnetic effects.

2. Considering an ideal CROME-like setup, the upper limit of the signal intensity is found to be just below the threshold of detectability.

3. Due to the relative weakness of the molecular bremsstrahlung signal compared to the geomagnetic signal, separation of the two will be difficult in the forward shower direction. AMBER- and MIDAS-like setups are better suited to search for an isotropic molecular bremsstrahlung signal, but the expected intensity of the signal might make direct detection impossible.

4. As far as the simulation itself is concerned, significant increases in accuracy could be achieved as better and more extensive descriptions or measurements of the ionization cross sections and momentum transfer cross sections of atmospheric molecules become available. It would also be worthwhile to explicitly include the effects of plasma dispersion in the computation.

Acknowledgements: This work has been supported by Federal Ministry for Education and Research (BMBF) Aspera-Grant 05A11VKA and the National Centre for Research and Development (NCBiR).

References

[1] J. Blümer, R. Engel, J.R. Hörandel, Prog. Part. Nucl. Phys. 63 (2009), 293 - 338.
[2] P. W. Gorham *et al.*, Phys. Rev. D78, 032007 (2008).
[3] P. Facal San Luis (Pierre Auger Collab.), Proc. of Int. Symposium on Future Directions in UHECR Physics, 13-16 February 2012 CERN; R. Gaior (Pierre Auger Collab.), these proceedings id 0883.
[4] R. Smida *et al.* these proceedings, id 0927, F. Werner *et al.* these proceedings, id 1112.
[5] L. Perrone, S. Petrera and F. Salamida, GAP-2005-87 (2005), Auger technical note.
[6] F. Nerling *et al.*, Astropart. Phys. 24, 6 (2006), 421 - 437.
[7] D. Gora *et al.*, Astropart. Phys. 24 (2006), 484-494.
[8] B. Rossi, High-Energy Particles, Prentice-Hall, 1952.
[9] S. Nijdam *et al.*, J. Phys. D: Appl. Phys. 44 (2011).
[10] P. W. Gorham, Astropart. Phys. 15 (2001), 177-202.
[11] G. Bekefi, Radiation Processes in Plasmas, Wiley, 1966.
[12] Y. Itikawa, J. Phys. Chem. Ref. Data 35, 1, (2006).
[13] Y. Itikawa, J. Phys. Chem. Ref. Data 38, 1, (2009).
[14] P. Neunteufel, Microwave Emission of Air Shower Induced Plasmas Due to Molecular Bremsstrahlung, Diploma Thesis, KIT, 2012.